Proc.4th Int. Conf. High Level Radioactive Waste Mgmt., 2061-2070, Las Vegas, April 26-30, 1993.

WETTING FRONT INSTABILITY IN AN INITIALLY WET UNSATURATED FRACTURE

M.J. Nicholl, R.J. Glass, and H.A. Nguyen
Geoscience Assessment and Validation Division 6115
Sandia National Laboratories
Albuquerque, NM 87185
(505) 844-0945

ABSTRACT

Experimental results exploring gravity-driven wetting front instability in a pre-wetted, rough-walled analog fracture are presented. Initial conditions considered include a uniform moisture field wetted to field capacity of the analog fracture and the structured moisture field created by unstable infiltration into an initially dry fracture. As in previous studies performed under dry initial conditions, instability was found to result both at the cessation of stable infiltration and at flux lower than the fracture capacity under gravitational driving force. Individual fingers were faster, narrower, longer, and more numerous than observed under dry initial conditions. Wetting fronts were found to follow existing wetted structure, providing a mechanism for rapid recharge and transport.

INTRODUCTION

When considering infiltration flow within an individual fracture above the water table in an arid environment, such as that at Yucca Mountain, Nevada, two initial conditions bound those expected. If the temporal separation between infiltration events is sufficiently long with respect to the time scale of matric imbibition, then the fracture will be essentially dry. Conversely, if events occur at times short with respect to matric imbibition, then wetted structure within the fracture will be wholly dependent on previous events. Closely spaced infiltration events could be associated with sequential storm fronts, such as the swarms of Pacific winter storms that regularly pass through the northern Sierra Nevada Mountains. Matric imbibition and evaporative redistribution will produce wetted structures between these bounding cases at intermediate times.

Dry initial conditions were considered by Nicholl et al.[1] in a study demonstrating gravity-driven wetting front instability at the cessation of slug infiltration within a transparent analog rough-walled fracture. Ponded infiltration analogous to that associated with intense rainfall in an arid region was simulated by applying a finite, distributed fluid slug to the upper boundary of the analog fracture. Redistribution of flow at the cessation of stable infiltration resulted in instability, which was manifested as the breakup of the coherent initial front into individual fingers (Figure 1). The leading edge of a finger consists of a coherent body of fluid, fully spanning the fracture aperture, which will be referred to as the finger-tip. As the finger-tip advances, it leaves behind fluid, wetting the fracture to field capacity. First-order theory was used to show that loss of fluid increases the capillary gradient opposing flow, causing the finger-tip to slow and eventually cease movement. The resultant wetted structure consists of alternating bands of wet and dry regions oriented in the direction of gravitational gradient (∇_g). The wetted bands are saturated to the field capacity of the analog fracture and terminate in stalled finger-tips (Figure 1d).

A second condition known to produce gravity-driven fingers in an analog rough-walled fracture under dry initial conditions is steady flux (q) at less than the gravity-driven saturated flux; defined as $K_s\nabla_g$, where K_s describes saturated hydraulic conductivity[1]. This boundary condition reflects a scenario where a low permeability layer such as a soil canopy supplies an underlying fracture by slow drainage. In such a scenario, individual fingers initiate from local heterogeneities along the material interface which act as point connections. Nicholl et al.[2] used a point source to simulate this boundary condition in an initially dry, rough-walled analog fracture consistent with their earlier work[1]. Finger-tip velocity and finger width were shown to be functions of the composite hydraulic properties of the system, fracture inclination, and flow rate.

Here we present laboratory experiments directed towards understanding infiltration behavior in a partially-saturated, inclined analog fracture. We begin with an overview of the experimental apparatus and transparent, rough-walled analog fracture. A procedure to uniformly wet the analog fracture to field capacity is then introduced. Experimental results demonstrating full-field instability in uniform moisture fields are presented. Measurements of single finger behavior under constant flow boundary conditions are compared to those taken under initially dry conditions. We then consider infiltration behavior in a structured moisture field resulting from previous infiltration flow instability. Existing wetted structure is observed to control the spatial path of subsequent infiltration events. Finally, we conclude with a hypothetical field scenario illustrating the significance of gravity-driven instability.

EXPERIMENTAL PROCEDURE

The experimental apparatus consisted of a rotating test stand (RTS), fracture test cell, and transmitted light visualization system. The analog aperture field was created by holding two roughened glass plates (60 x 30.5 cm) in close contact through application of a confining pressure (20 psi). All boundaries were held open to atmospheric pressure. Mean aperture ($\tilde{a}$ = 0.0225 cm) of the test fracture was measured by volumetric imbibition. Saturated conductivity (K_s) of a smaller

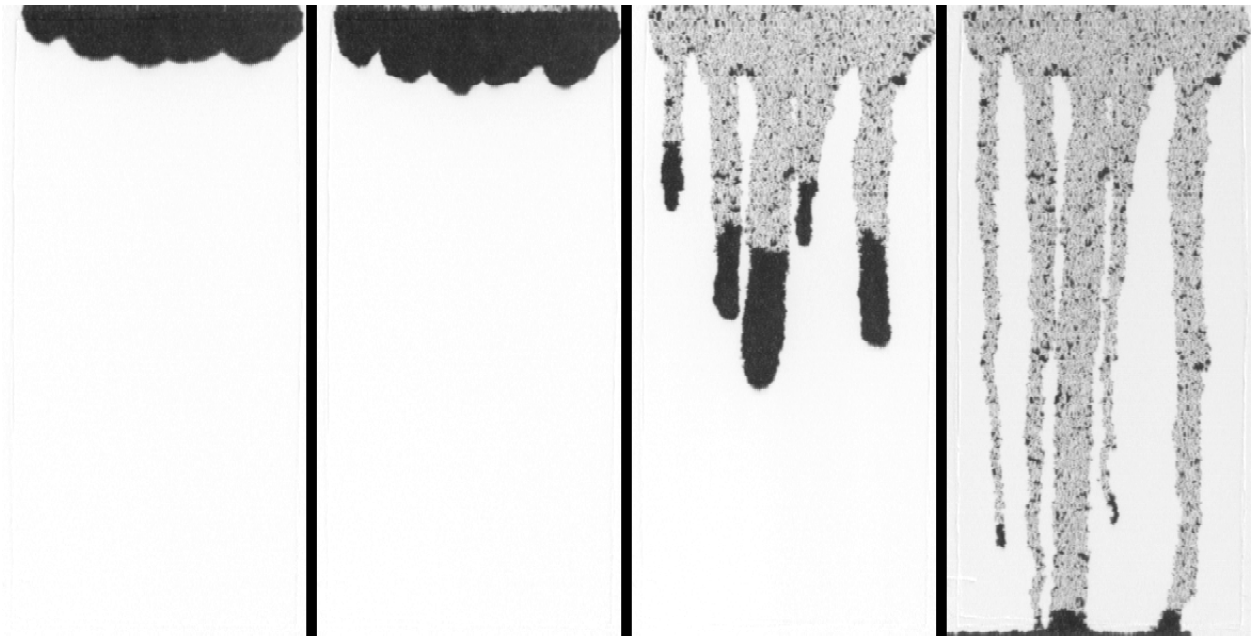

a) b) c) d)

Figure 1: Sequence illustrating the development of instability in an initially dry fracture (∇_g = 1.00, L_i = 6.25 cm): a) Advancement of stable front (t = 1s); b) Onset of instability, note drainage along upper boundary (t = 2s); c) Development of fingers (t = 8s) note the velocity differential between small and large fingers (t = 15s); d) The two smallest fingers (numbers 1 and 4, counting from the left) have ceased movement (t = 61 minutes).

analog fracture (30.48 x 15.24 cm, ã = 0.0213 cm) constructed from the same material was reported as 188 cm/minute[2]. By utilizing parallel-plate-law assumptions, those results may be extended to the analog fracture used in these experiments, yielding K_S = 209 cm/minute. Data was acquired in the form of digital images, obtained at 512 x 512 pixel and 256 gray level resolution. Thorough descriptions of both the experimental apparatus and analog fracture are provided in Nicholl et al.[1].

Uniform Initial Moisture Field

A procedure was developed to produce a uniformly wetted moisture field within the analog fracture. The RTS was first inclined, locating the upper boundary of the test fracture slightly lower than the bottom boundary (~5 cm). Fluid was applied to a point source on the upper boundary from a hand syringe; manual control of the flow rate was used to maintain a balance between capillary and gravitational forces, producing a uniform wetting front. After the test fracture was fully saturated, the RTS was rotated, bringing the fracture plane to the test inclination. The saturated test fracture was then allowed to drain freely until it reached a stable condition. The capillary fringe along the bottom boundary was then evacuated with an absorbent towel. The resultant moisture field was wetted at the field capacity of the analog fracture (Figure 2a,b). Experiments were conducted immediately after drainage to minimize potential evaporative effects along the boundaries.

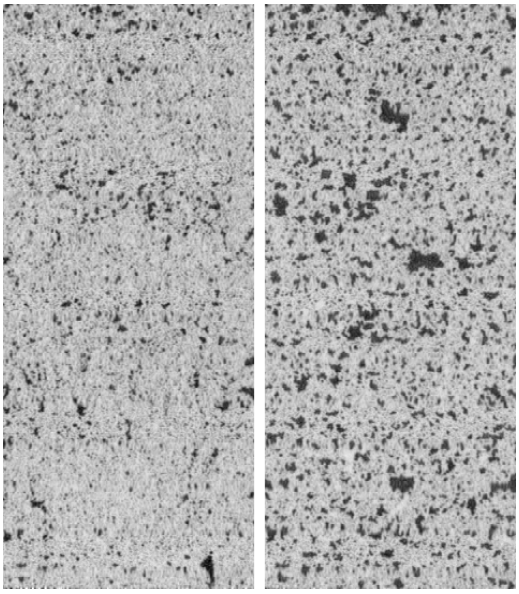

a) b)

Figure 2: Effects of gravitational gradient on field capacity of the analog fracture: a) ∇_g = 1.00; b) ∇_g = 0.25.

TABLE 1

Full-field experiments performed in a pre-wetted fracture

Exp. #	∇_g	L_i (cm)	Initial Moisture Field (L_i in cm)
mult14	1.00	5.00	*
mult16-2	1.00	5.25	20.49
mult25p	1.00	6.12	6.27
mult13-2	1.00	7.56	8.99
mult9p	1.00	9.91	10.32
mois7	1.00	10.45	*
mois8	1.00	10.78	*
mult15	1.00	10.93	*1
mult24p	1.00	24.25	24.26
mult26p	1.00	28.97	28.4
mult27p	1.00	33.57	33.95
mult12-3	0.75	5.46	33.47[2]
mult12-2	0.75	5.79	33.47
mult11p2	0.75	9.43	28.17[3]
mult10p	0.75	18.89	18.68
mult11p	0.75	28.11	28.17
mult44p	0.75	38.09	37.95
mult28p	0.50	5.83	5.39
mult3	0.50	9.88	9.85
mult29p	0.50	13.41	14.4
mult30p	0.50	18.96	19.38
mult31p	0.50	20.95	21.84
mois5	0.25	10.17	*
mult45p	0.25	15.01	14.41
mult46p	0.25	19.6	19.21
mult47p	0.25	24.95	23.75
mult48p	0.25	29.06	28.91
mult43p	0.25	33.37	33.37

Experiments were performed at arbitrary intervals during two separate experimental sequences (mult and mois). L_i is defined as the height of the fluid column applied to the analog fracture and is equal to the volume of fluid applied ,divided by the average cross sectional area of the analog fracture. The initial moisture field was created by unstable infiltration (input = L_i) under initially dry conditions; with the following exceptions:

* - a uniformly distributed initial moisture field was used .
1 - initial field was created prior to experiment 14 and then reused for this experiment.
2 - initial field was created prior to experiment 12-2 and then reused for this experiment.
3 - initial field was created prior to experiment 11p and then reused for this experiment.

TABLE 2

Single fingers initiated from a point source

Exp. #	∇_g	Q (ml/minute)	v (cm/minute)	W (cm)
mois10	1.00	0.035	22.4211	0.831
mois9	1.00	0.0591	23.3513	0.614
mois11	1.00	0.0609	18.9817	0.587
mois12	1.00	0.0684	21.0538	0.572
mois14	1.00	0.334	54.2807	0.799
mois13	1.00	0.3442	38.168	0.826
mois15	1.00	0.3635	40.3229	0.829
mois23	1.00	0.7	71.7456	0.831
mois22	1.00	0.8034	61.5807	0.609
mois18	1.00	1.5903	91.4545	1.122
mois17	1.00	1.807	96.9006	1.345
mois16	1.00	1.8783	*	1.24
mois24	1.00	2.5254	*	1.736
mois19	0.75	0.0648	24.5634	0.623
mois20	0.75	0.0675	20.0228	0.786
mois21	0.75	0.0717	16.5632	0.605
mois25	0.75	0.3419	36.7289	0.745
mois26	0.75	1.8324	72.7729	1.225
mois29	0.50	0.0665	12.0914	0.8
mois30	0.50	0.359	26.2287	0.954
mois31	0.50	1.68	56.4036	1.892
mois4	0.25	0.0363	2.6596	1.373
mois1	.25	0.0639	#	#
mois2	0.25	0.0662	5.3368	1.478
mois3	0.25	0.073	6.4134	1.148
mois27	0.25	0.3486	13.1584	1.86
mois28	0.25	1.7908	31.1933	3.424

* - finger was not stable for a large enough interval to measure velocity

\# - This experiment was performed in a structured field created by inverting a partially filled fracture. As it is inconsistent with the other experiments no measurements are reported.

Experimental Fluid

Because data was acquired by digital imaging techniques, the experimental fluids were dyed to provide enhanced visual contrast. In the experiments presented here, three different fluids were used: pure de-ionized water (DI), a high-contrast fluid, and a low-contrast fluid. In all experiments, the high-contrast fluid was used as the infiltrating fluid. High contrast fluid was also used to form the initial moisture field in the first series of experiments; associated problems discriminating between the advancing front and initial moisture field led to the use of either DI or low contrast fluid to form the initial moisture field in subsequent experiments. At early times, delineation of the advancing front was greatly improved; however, as the experiment progressed, mixing between the fluids tended to smear the leading edge of the front. As finger-tips contact a higher volume of the initial fluid than do the finger sides, mixing was most pronounced at the finger-tip. The high contrast fluid was composed of 1 liter DI mixed with 1 g each of FD&C Blue #1 and Red #3 dyes; the low contrast fluid was composed of 1 liter DI mixed with 0.125 g each of the same dyes. Capillary properties of all three fluids were evaluated in glass capillary tubes and found to be consistent. Density differences between the fluids were on the order of 0.2%. As the primary displaced fluid was air, density differences between the infiltrating and initial liquids had a lower order effect on flow and therefore, these effects were assumed to be negligible.

RESULTS

A series of experiments were conducted in an analog fracture under pre-wetted conditions. Parameters varied were limited to ∇_g, initial moisture field, inflow boundary condition, and the amount of fluid applied to the fracture. Gravitational gradient was varied by positioning the RTS such that the fracture was inclined from vertical at angles of 0, 41.5, 60, and 75.5 degrees; corresponding to ∇_g of 1.0, 0.75, 0.50, and 0.25. Results are presented in two sections, one for each of the initial conditions explored. Behavior in a moisture field uniformly wetted to field capacity is considered first. Experiments performed in structured moisture fields created by previous unstable infiltration events are presented in the second section. Two boundary conditions known to produce instability in initially dry fractures[1] were implemented; cessation of stable infiltration and steady flow at less than $K_s\nabla_g$. Results are summarized by boundary condition in Tables 1 and 2.

Uniform Moisture Field

Experiments presented in this section were performed in moisture fields uniformly wetted to field capacity of the analog fracture. Field capacity describes the amount of fluid retained by the fracture at the cessation of free gravitational drainage. During drainage, competition between capillary and gravitational forces controls fluid movement. Gravity acts as a body force on the fluid as a whole, while capillary forces vary spatially in response to changes in the aperture field. Where the aperture is sufficiently small, capillary forces restrain fluid from drainage. As gravitational force is decreased, the aperture size capable of retaining fluid is expected to increase. As a result, moisture content and wetted area of the fracture are also expected to increase. Images illustrating differences in wetted area at field capacity are shown as Figure 2. Wetted area of the fracture at small ∇_g (0.25, Figure 2b) appears to be greater than that at large ∇_g (1.00, Figure 2a), implying an increase in moisture retention.

full-field instability

This section considers the redistribution of flow following the application of a finite slug along the upper boundary of the analog fracture. During imbibition, capillary forces along the leading edge of the front act to reinforce gravity, thereby serving to stabilize flow. When the input slug is exhausted and drainage begins, the capillary gradient then reverses direction to oppose flow. This leads to a de-stabilization of the front and the development of fingers[1].

A stable infiltration front is produced by simultaneously injecting the contents of 16 evenly spaced syringes along the upper boundary of the analog fracture. A reservoir enclosing the fracture boundary allows ponding of excess fluid when input rate exceeds the imbibition capacity of the fracture. This procedure produces a boundary condition analogous to the surface ponding associated with a sudden precipitation event. The amount of fluid applied to the fracture is expressed as a length (L_i), defined as the average volume of fluid applied per unit cross-sectional area of the fracture (fracture width multiplied by mean aperture). Five experiments were performed, four at $\nabla_g = 1.00$ and one at $\nabla_g = 0.25$ (Table 1). Fluid was applied with the intent of minimizing perturbations but without attempting to form a completely flat front.

A typical experimental sequence is shown in Figure 3. This experiment can be directly compared to the one shown in Figure 1, as the small difference in L_i (6.25 cm in Figure 1, 5.00 cm in Figure 3) has a lower order effect on flow behavior than that of moisture within the analog fracture (dry in Figure 1, wetted to field capacity in Figure 3). Prior to the onset of instability (Figure 3a), the stable front exhibits a very complex structure containing a substantial volume of entrapped air. Observed behavior contrasts significantly with the fully saturated fronts dominated by long-wavelength features that are characteristic of dry initial conditions (Figure 1a). The front becomes unstable at the onset of redistribution, with fingers forming from the most significant perturbations (Figure 3b). As there are numerous features at short wavelength in the pre-wetted fracture, the number of fingers formed (Figure 3c) is larger than in the dry fracture (Figure 1c). Finger-tips in the unstable front (Figure 3d) are longer and narrower than in the dry experiments. Fingers display a more uniform advancement than in the dry fracture, where the smaller fingers are noticeably slower than the large fingers. In the pre-wetted fracture, adjacent fingers repeatedly merged and split; while fingers readily merge under initially dry conditions, splitting is rarely observed. Complexity of the system dynamics precludes measurement of individual finger behavior.

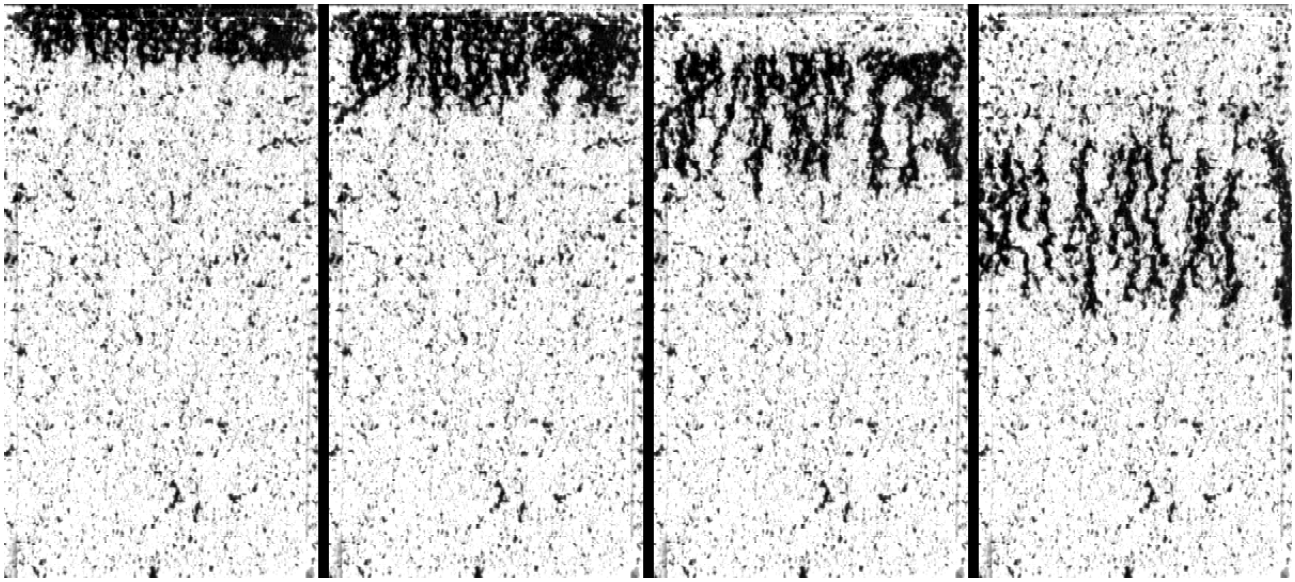

a) b) c) d)

Figure 3: Sequence illustrating the development of instability in a fracture uniformly wetted to field capacity. The dark region along the bottom boundary consists of undrained capillary fluid (∇_g = 1.00, L_i = 5.00 cm): a) Advancement of stable front, note complexity, small wavelength features, and air entrapment (t = 2s); b) Onset of instability, note drainage along upper boundary (t = 4s); c) Development of fingers, note connection between adjacent fingers and number of fingers (t = 8s); d) Further advancement, note relatively uniform advancement of adjacent fingers as compared to Figure 1c (t = 15s).

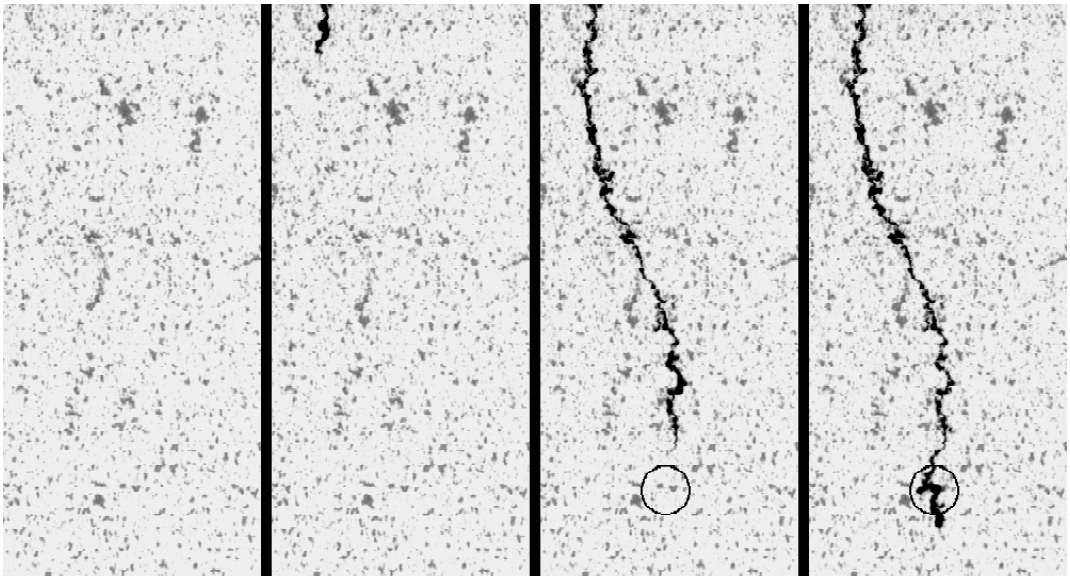

a) b) c) d)

Figure 4: Single finger initiated from constant flux boundary condition (∇_g = 0.50, Q = 0.0665 ml/minute): a) Initial moisture field; b) Instigation of finger from point source; c) Advancement of finger through the moisture field, note the two fluid clusters circled; d) Translation of finger path after contact with the clusters in Figure 4c.

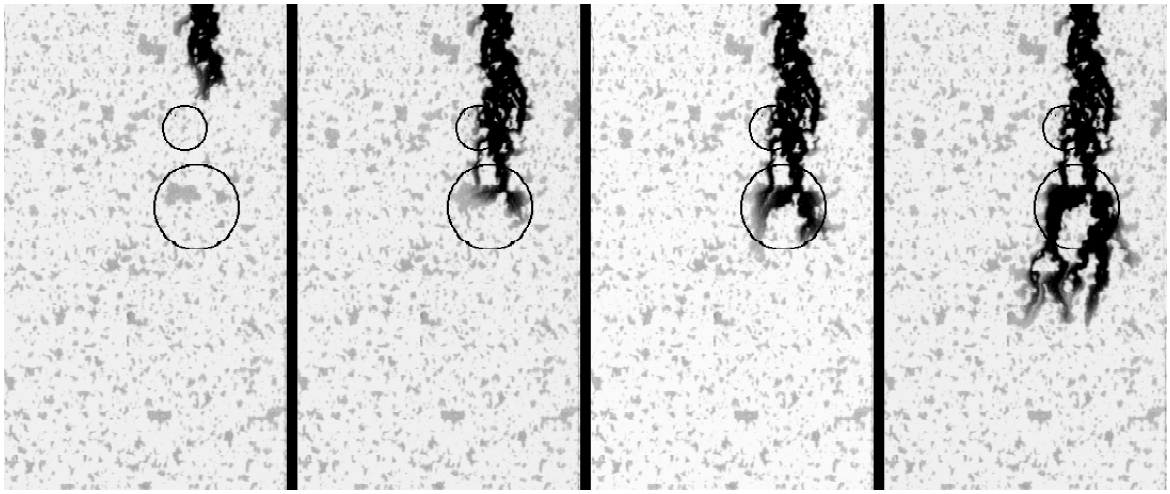

a) b) c) d)

Figure 5: Finger splitting caused by a perturbation (∇_g = 0.25, Q = 1.791 ml/minute): a) Initial formation of the finger. Note the circled fluid clusters; b) Finger has developed a dendritic sub-finger associated with clusters in the upper circle and has just contact clusters in the lower circle; c) Finger splits at lower clusters; d) Additional splitting and merging occurs.

single fingers from a point source

Individual fingers were initiated by supplying steady flow from a syringe pump to a point source on the upper boundary of the analog fracture; see Nicholl et al.[2] for additional experimental details. Volumetric flow rate (Q) was varied over the range from 0.035 ml/minute to 2.5 ml/minute; results are summarized in Table 2. The lower limit on Q was set by the ability of the syringe pump to provide a stable flow rate. The upper limit was set by the ability of the partially saturated fracture to imbibe fluid and form a single finger within the analog fracture. As Q was increased, fingers tended to split into multiple sub-fingers as discussed below; thereby limiting our ability to take meaningful measurements. The upper limit on volumetric input is considerably lower than was possible in a similar analog fracture under dry initial conditions[2], particularly at large ∇_g.

The advance of a typical finger through the partially wetted analog fracture is shown in Figure 4. The initial moisture field is shown in Figure 4a and the initiation of the finger in Figure 4b. As the finger advances down-gradient (Figures 4c,d) it repeatedly encounters clusters of spanned apertures that act as instantaneous perturbations to the finger-tip. These perturbations were noted to have a significant effect on the actual path of the finger. The advancing finger illustrated in Figure 4 contacted two such clusters virtually simultaneously (circled on Figure 4c). The result was a translation of the flow path in a direction off gravitational gradient (Figure 4d). Splitting and merging of fingers could also be induced by contact with in-place fluid clusters as illustrated in Figure 5. While fingers travel primarily in the direction of ∇_g, the exact path of the finger appears to be very sensitive to the initial conditions.

finger-tip velocity

Finger-tip velocity (v) was defined as the rate of change in position of the leading edge of the saturated tip, measured in the direction of gravitational gradient. Local fluctuations, boundary effects, dissipative sub-fingers, and fluid mixing at the tip all complicated measurement of velocity. Contact with in-place fluid clusters perturbs the finger-tip, leading to local velocity fluctuations. To obtain a stable estimate of finger-tip velocity, measurements were averaged over the largest length scale possible for the experiment in question. Dendritic sub-fingers, such as that seen in Figures 4 and 5 are dissipative features that are often of a transitory nature. As such, they were avoided during the measurement process. As previously discussed, the invading fluid and initial moisture field contained differing concentrations of dye. Hence, mixing tended to obfuscate the leading edge of the finger-tip; an effect that increased with finger advancement. Measurements were not made unless the leading edge could be distinctly identified.

Experimental observations of tip velocity in the pre-wetted analog fracture are shown as a function of Q in Figure 6. The data plot on four distinct curves, one for each ∇_g studied. Data exhibit a form similar to that reported by Nicholl et al.[2] for single fingers in a comparable analog fracture under dry initial conditions. In that study, dimensionless velocity (R_v) was observed to display a relationship with dimensionless flux (R_q) of the form shown below:

$$R_v/\nabla_g = f(R_q/\nabla_g) \quad (1)$$

where:

$$R_v = v/(K_s\nabla_g) \quad (2)$$

$$R_q = Q/(\tilde{a}K_s\nabla_g W_f) \quad (3)$$

where W_f is the measured finger width. Data collected from pre-wetted fractures appear to be consistent with this functional form, collapsing towards a single curve. Transformed data are shown in Figure 7 along with data collected under initially dry conditions. The 1:1 line indicates equivalence between R_v and R_q. Fingers in the pre-wetted fracture display a similar functional form to those collected in the dry fracture but at a consistently higher velocity.

finger-width

Finger width (W_f) was defined as the average width of the region swept by the advancing finger-tip, measured perpendicular to ∇_g. Referring to the discussion under tip velocity, measurements of finger width were made over the largest possible stable region. Finger width is shown as a function of volumetric input in Figure 8. Data collected at low ∇_g (0.25 and 0.50) appear to follow separate linear trends, each rising with Q from its' respective minimum finger width. Data collected at large ∇_g (0.75 and 1.00) appear to plot along a single line, with a smaller minimum width and gentler slope.

Data collected at low Q (<1 ml/minute) and large ∇_g (>0.25) do not differ significantly from a constant value ($W_f \sim 0.75$ cm). As the finger advances, it repeated contacts clusters of spanned apertures which act as instantaneous, finite perturbations to the finger-tip. Repeated perturbations of similar size could cause the finger width to tend toward the average cluster width. However, even though mixing was less apparent along finger sides than at the tip, it did complicate delineation of the finger boundary. As a result, systematic measurement error cannot be completely dismissed as a possible explanation.

Finger width may be expressed in dimensionless form as relative width (R_w), defined as the portion of the fracture width (S_w) occupied by the finger. Relative flow (R_i) is defined as the ratio between Q into the finger and gravity-driven saturated flow through a section of width S_w. In a similar but dry analog fracture[2], R_w was observed to display a functional relationship with R_i.

$$R_w = f(R_i) \quad (4)$$

where:

$$R_w = W_f/S_w \quad (5)$$

$$R_i = Q/(\tilde{a}K_s\nabla_g S_w) \quad (6)$$

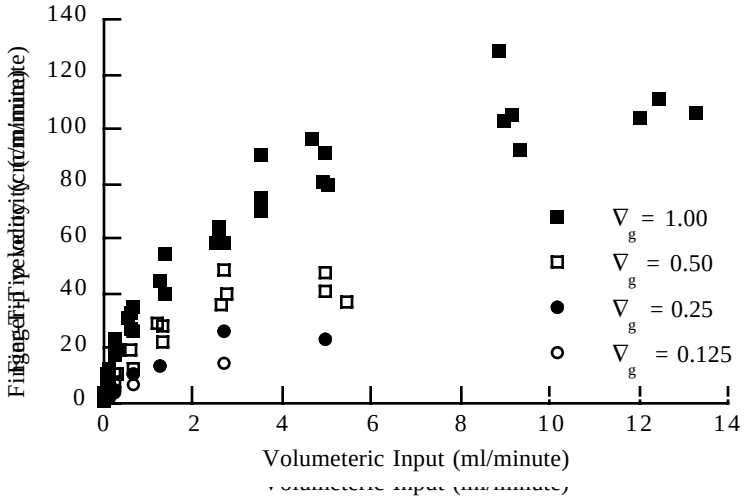

Figure 6: Measured finger-tip velocity: Measurements plot on four distinct curves corresponding to the four fracture inclinations studied; 0, 41.5, 60, and 75.5 degrees from vertical, corresponding to ∇_g of 1.0, 0.75, 0.50, and 0.25, respectively.

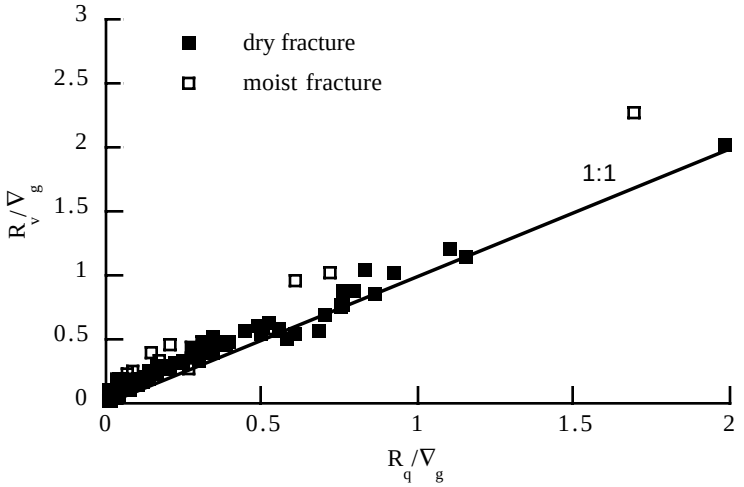

Figure 7: Dimensionless tip velocity as a function of dimensionless flux: Data collected under dry initial conditions (dark squares) is shown for comparison.

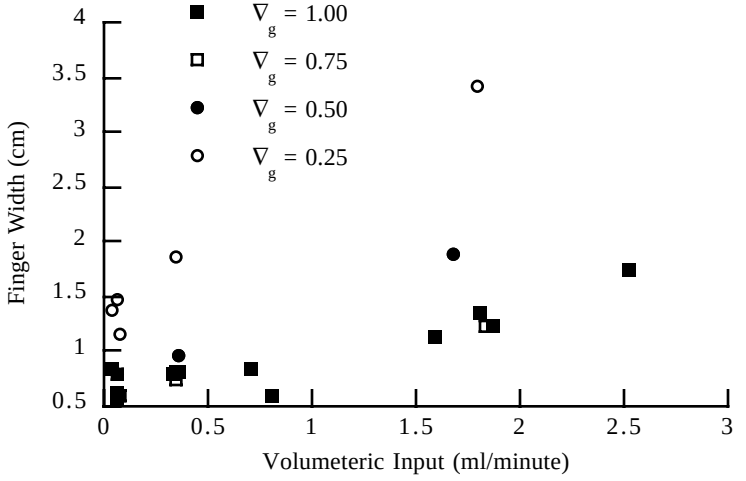

Figure 8: Measured finger width: Data appears to plot along three lines, points associated with large ∇_g (1.00 and 0.75) are mixed. Not the region at low Q and large ∇_g where W_f appears to be constant.

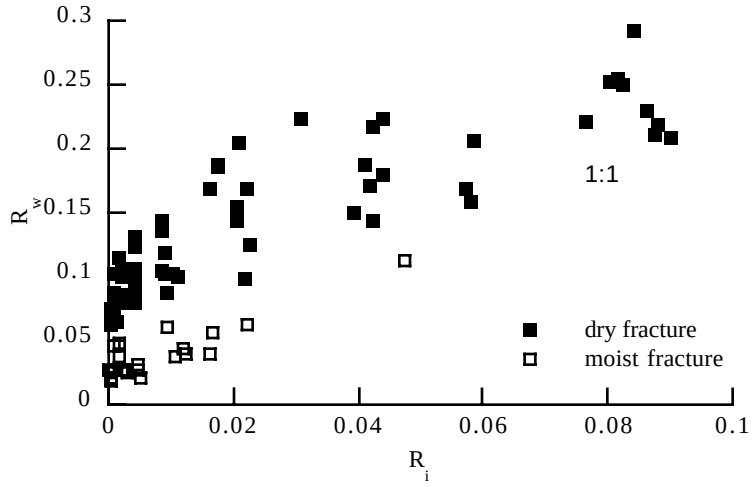

Figure 9: Dimensionless width as a function of dimensionless flow: Data collected under dry initial conditions (dark squares) is shown for comparison.

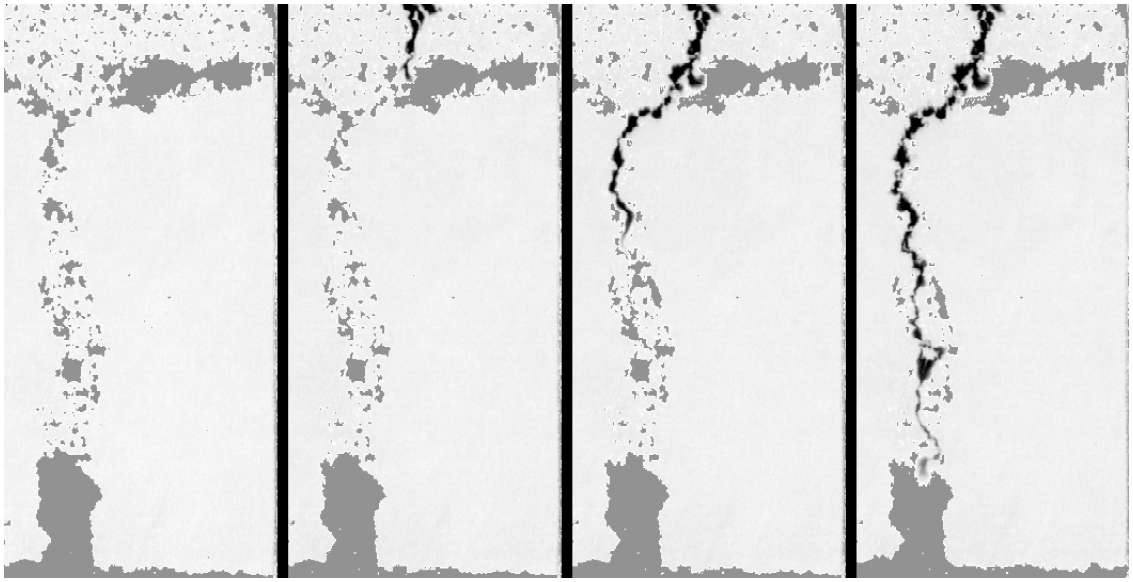

a) b) c) d)

Figure 10: Channeling of an individual finger by a non-uniform moisture field (∇_g = 0.25, Q = 0.0639 ml/minute): a) Non-uniform initial moisture field; b) Initiation of the finger. The finger moves primarily in the direction of ∇_g in the relatively uniform portion of the field; c) Finger preferentially follows wetted structure; d) Finger continues to remain within pre-wetted zone.

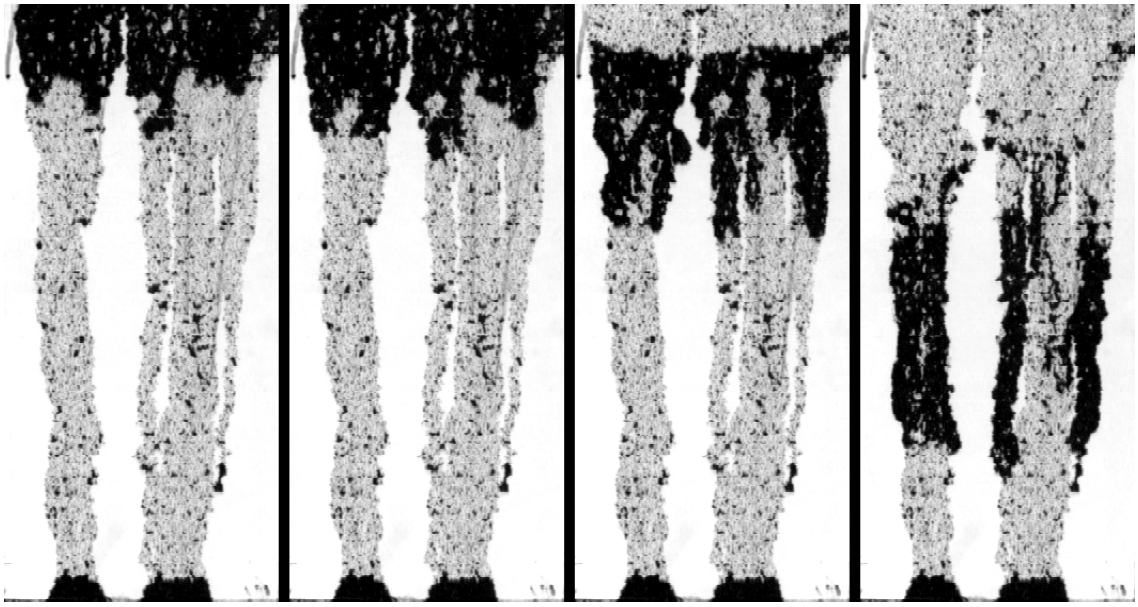

a) b) c) d)

Figure 11: Channeling of distributed infiltration front by a non-uniform moisture field (∇_g = 0.25, L_i = 7.56 cm): a) Stable infiltration within the initial moisture field; b) Onset of instability, note complicated structure of the front; c) Fingers continue to advance within the existing moisture field; d) Adjacent fingers on the left hand side have merged into a single unit.

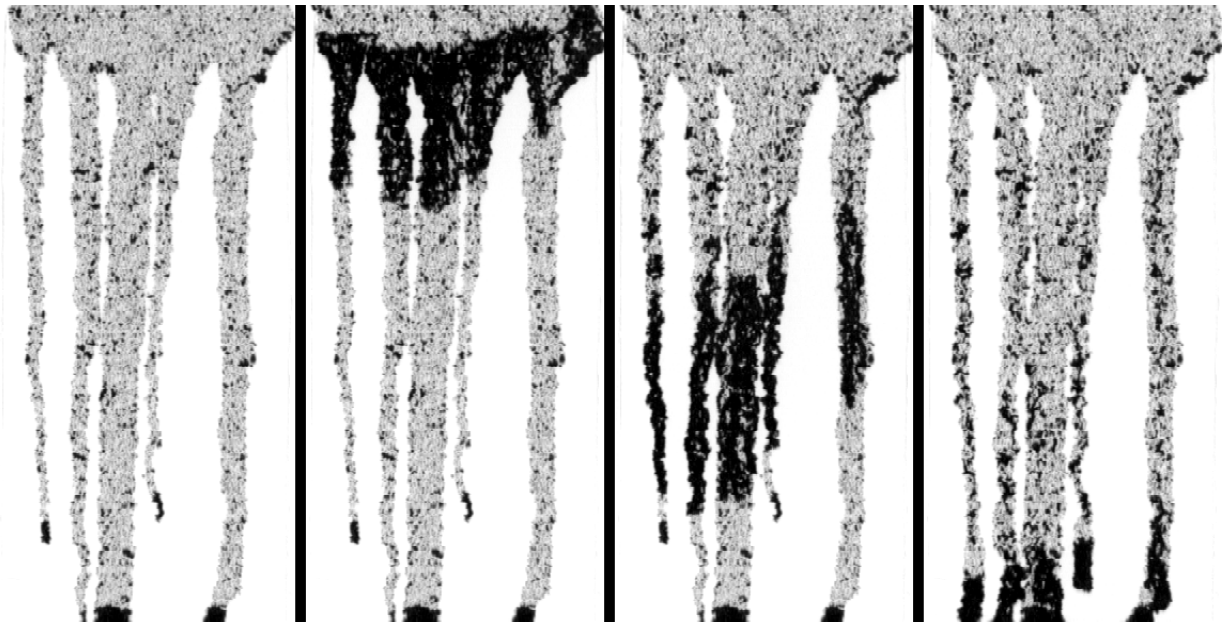

a) b) c) d)

Figure 12: Re-start of stalled fingers (∇_g = 0.50, L_i = 6.12 cm): a) Initial moisture field, three fingers have spanned the system and two have stopped showing no movement for 60 minutes; b) Infiltration of a second front; c) Again the second front is constrained to the existing moisture field; d) Fluid reaches the stalled finger tips causing them to resume advancement through the fracture.

As S_w is not a characteristic length associated with the flow process, it may be chosen arbitrarily. The analog fracture used by Nicholl et al.[1] to explore individual fingers under dry initial conditions had a width of 15.24 cm; in order to directly compare those results with the experiments presented here, S_w was assigned a value of 15.24 cm. Re-scaled data are presented as Figure 9. Within the range of R_i considered in these experiments, data from both sets of experiments tend to increase from a minimum width with relative flow. Fingers measured in the pre-wetted fracture appear to be generally narrower than those observed in a similar fracture under dry initial conditions.

Non-Uniform Wetted Structure

Fracture conductivity and capillary pressure are both strongly non-linear functions of saturation; therefore, a non-uniform wetted structure is expected to have a significant influence on infiltration. The wetted structure created by an unstable infiltration front consists of the partially saturated paths left by the fingers, ending in stalled finger-tips (Figure 1d). The partially saturated regions are wetted to field capacity of the analog fracture. At times short with respect to matrix imbibition and evaporative redistribution, such wetted structures serve as the initial condition for subsequent infiltration.

The initial moisture field seen in Figure 10a was formed through inversion of a partially filled fracture; this technique is commonly used to produce an unstable density stratification in smooth-walled Hele-Shaw cells (e.g. [3]). Fluid was applied at a constant rate from a point source located at the center of the analog fracture. Where the moisture field was relatively uniform, motion of the resultant finger was primarily in the direction of ∇_g (Figure 10b). After passing through the uniformly wetted zone, the finger preferentially follows the existing wetted structure (Figure 10c,d). It is hypothesized that this apparent channeling is associated with the wetting properties of the system. The in-place fluid clusters, seen as dark regions, are areas where the fracture aperture is fully spanned. The small contact angle of water in the experimental system (glass/air) causes the actual domain of these clusters to be considerably larger. When an advancing finger contacts the film surrounding such a cluster, the contact angle goes to zero and flow moves in the direction of the cluster. Similarly, when a cluster is contacted it becomes part of the finger and expands. In doing so, its outer boundary will contact the film surrounding other clusters, causing flow to move in that direction. In this manner, even if the in-place fluid clusters are fully disconnected, flow will tend to follow the pre-wetted domain. If the clusters are uniformly distributed, then wetting effects will tend to cancel out, causing flow to be more directly aligned with gravitational gradient.

A series of full-field experiments were performed using the slug-input boundary condition described previously (Table 1). After running an experiment in an initially dry fracture, the system was allowed to drain to a short-term stable condition prior to application of a second fluid slug. In all cases, the second front was observed to preferentially follow the existing wetted structure; a typical experimental sequence is illustrated in Figure 11. As was seen in uniform moisture fields, prior to the onset of instability the stable front contains a substantial volume of entrapped air and exhibits structure at all wavelengths above aperture scale (Figure 11a). The stable front preferentially follows the existing wetted structure. After the onset of instability (Figure 11b), the front breaks up into individual fingers within the existing wetted structure (Figure 11c). Fully developed fingers continued to follow the wetted structure (Figure 11d); note that adjacent fingers on the left hand side appear to have merged. In such structured moisture fields, finger merging appears to be more common than splitting, as the hydraulic boundary created by the initial moisture structure tends to concentrate fingers. As was observed in uniform moisture fields, fingers were longer, narrower, and exhibited more structural complexity than was observed in the initially dry experiments.

re-start of stalled finger-tips

When the existing moisture field is wetted to field capacity, subsequent infiltration events traveling through that field are expected to lose little fluid during passage. The net effect is that the bulk of the front is rapidly transferred to the stalled finger-tips from the previous event. Figure 12a shows the wetted structure in an initially dry fracture sixty-one minutes after application of a finite slug. Of the five fingers initially formed, three span the fracture and two stalled in place. After ascertaining that the structure was stable, a second front of similar magnitude was applied (Figure 12b). Flow through the wetted structure was confined to the existing moisture field (Figure 12c). A significant portion of the flow volume reached the stalled tips, restarting their movement (Figure 12d). If the analog fracture had been larger, similar behavior would have been expected in all five fingers. After the finger-tips resume movement they will be advancing through a dry zone. As a result, the finger-tips will lose fluid by wetting the fracture, causing them to lose velocity and eventually stall again.

CONCLUSIONS AND DISCUSSION

Initial wetted structure within a rough-walled analog fracture has significant effects on subsequent infiltration events. Wetting front instability was demonstrated both in uniform moisture fields wetted to field capacity and structured fields created by previous unstable infiltration. Fingers were observed to be longer, faster, narrower, and more complicated structurally than was observed in initially dry fractures. Pre-existing wetted structure controls infiltration behavior at two scales. In general, flow follows and is constrained within the existing wetted structure. At a smaller scale, finger behavior is related to the spatial structure of individual fluid clusters. Small clusters of spanned apertures within the fracture act as instantaneous perturbations to advancing fingers, affecting the fingers' path, tip velocity, structure, and width. Adjacent fingers often split or merge; this behavior is often associated with in-place fluid clusters.

The significance of wetting front instability can best be illustrated through the use of an idealized field scenario. Consider an unsaturated, low-permeability rock unit containing extensive, non-horizontal, dry fractures outcropping at the surface. On cessation of imbibition into the fractures after an intense rainfall event, the advancing front within the fractures becomes unstable. Finger-tips transport water and solutes downward, leaving a path wetted to field capacity. As the finger-tip loses fluid it slows and eventually comes to a halt. Because less area of the fracture is wetted, the unstable front will have advanced significantly further than would be expected for a stable front of equal magnitude. If a subsequent rainstorm occurs in a time frame short with respect to matrix imbibition, the existing wetted structure will provide a preferential pathway directing the second infiltration front to the stalled fingertips from the preceding event. As the existing moisture field is wetted to field capacity, fluid loss is expected to be minimal; hence, virtually the entire second front is transferred to the stalled finger-tips, which then resume movement. This mechanism would promote rapid recharge and transport of solutes through a fractured formation.

When combined with other studies[1,2], the work presented here provides a basic conceptual understanding of gravity-driven infiltration instability in an unsaturated, homogeneous analog fracture. Additional work is necessary for the inclusion of wetting front instability into conceptual models of unsaturated fracture flow. Heterogeneity driven channeling has been shown to occur in saturated fractures[4,5]. This process is expected to compete with gravity-driven instability in controlling flow structure in an inclined, unsaturated fracture. The authors currently are planning systematic experimentation to evaluate the effects of aperture heterogeneity on gravity-driven instability. Experiments will be performed in both epoxy casts of natural fractures and manufactured aperture fields. Another important consideration is fracture/matrix interaction; Glass and Tidwell[6] used an analog half-plane system to demonstrate that matrix imbibition does not significantly inhibit finger development. Finally, the work of Glass[7] regarding the inclusion of gravitational and surface tension effects into pore scale modeling techniques provides a basis for numerical experimentation that will be further explored.

ACKNOWLEDGMENTS

The authors gratefully acknowledge the assistance and support provided by the following: W.C. Ginn in design and fabrication of the experimental apparatus; L. Orear in development of image acquisition software; P.B. Davies, J.H. Gauthier, and V.C. Tidwell for their careful and constructive reviews. This work was supported by the U.S. Department of Energy, Office of Civilian Radioactive Waste Management, Yucca Mountain Site Characterization Project Office, under contract DE-AC04-76DP00789.

REFERENCES

1. M.J. NICHOLL, R.J. GLASS, and H.A. NGUYEN, "Gravity-Driven Fingering in Unsaturated Fractures", Proceedings of the Third Annual International Conference on High Level Radioactive Waste Conference, Las Vegas, Nevada, April 12-16, (1992).

2. M.J. NICHOLL, R.J. GLASS, and H.A. NGUYEN, "Small-Scale Behavior of Single Gravity-Driven Fingers in an Initially Dry Fracture", Proceedings of the Fourth Annual International Conference on High Level Radioactive Waste Management, Las Vegas, Nevada, (1993).

3. T. MAXWORTHY, "The Nonlinear Growth of a Gravitationally Unstable Interface in a Hele-Shaw Cell", J. Fl. Mech., 177, 207-232 (1987).

4. I. NERETNIEKS, T. ERICKSEN and P. TAHTINEN, "Tracer Movement in a Single Fissure in Granitic Rock: Some Experimental Results and their Interpretation", WRR, 18, 849-858, (1982).

5. I. NERETNIEKS, "Solute transport in fractured rock - Applications to radionuclide waste repositories", SKB Technical Report 90-38, Swedish Nuclear Fuel and Waste Mnagement Co., (1990).

6. R.J. GLASS and V.C. TIDWELL, "Research Program to Develop and Validate Conceptual Models for Flow and Transport Through Unsaturated, Fractured Rock,"Proceedings of the Second Annual International Conference on High Level Radioactive Waste Management, April 28-May 3, 1991, Las Vegas, Nevada, 977-987, (1991).

7. R.J. GLASS, "Modeling Gravity Driven Fingering Using Modified Percolation Theory", Proceedings of the Fourth Annual International Conference on High Level Radioactive Waste Management, Las Vegas, Nevada, (1993).